Heat transport modelling and adaptive model predictive temperature control of the direct current plasma nitriding process performed in a linear non-isotherm plasma reactor

Nimród D. Kutasi*, Emőd Filep*, Lajos Kenéz*

* *Department of Electrical Engineering, Faculty of Technical and Human Sciences, Sapientia-Hungarian University of Transylvania, Tg. Mureş, (e-mail: kutasi@ms.sapinetia.ro, efilep@ms.sapientia.ro, l_kenez@ms.sapientia.ro).*

Abstract: The paper focuses on the exact modelling and the model-based predictive temperature control of the direct current plasma nitriding (DCPN) system. The DCPN process is a well-known industrial technology, however the mathematical modelling of the process from the control point of view is not developed, thus the aim of the paper is to develop a systematic modelling procedure for the heat transport and pressure dynamics. The heat transport modelling was performed taking into account the heat transported by the gas-flow, the conducted heat and the radiated heat. The emissivity of the treated part was estimated and the temperature dependence of the emissivity was modelled. The pressure dynamics was modelled and validated. The obtained model for the temperature dynamics is highly nonlinear, mainly due to the heat-radiation, and the model contains variable parameters like the mass of the treated parts, thus an adaptive model predictive controller (A-MPC) is proposed for an accurate temperature control. The performance of the A-MPC is compared with the classical PID controller, proving the benefits of the model-based control.

Keywords: plasma nitriding, heat transfer, nonlinear model, model predictive control, adaptive control.

1. INTRODUCTION

The plasma nitriding is one of the most developed heat-treatment technology, it is used when the induction heating is inappropriate due to the deformation of the treated part, or when special hard thin layer is requested on the surface of the part. There are two major plasma nitriding technologies, the classical direct current plasma nitriding (DCPN) and the active screen plasma nitriding (ASPN). From control point of view, there are several process variables that need accurate control, the most important are the temperature of the treated part and the reactive gas pressure and composition, (Rembges et al., 1993), (Szatyapal et al., 2013). The control of the forementioned process variables are similar for both technologies, in this article the modelling and control of the DCPN process is developed.

There are several articles dealing with the modelling of the plasma nitriding process, but all of them presents the model of the layer formation during nitriding for a certain process condition. In (Cavaliere et al., 2009), the thermo-chemical diffusional process of the nitriding is developed. In (Guiberteau et al., 1997) the pulse glow discharge is modelled. The nitriding process is described in detail in (Kenéz et al., 2013) or (Mittemeijer, 2013). Closed loop control of the layer formation in the nitriding (salt bath nitriding) process, layer thickness measurement is presented in (Ratajski et al., 2008, 2009). From process control point of view, (Rembges et al., 1993) presents general aspects of the nitriding process control, (Filetin et al., 2005).

To overcome the nonlinear nature of the process, (Oltean et al., 2014) proposed artificial intelligence for the process control, namely a fuzzy logic based temperature control.

The goal of this article is to develop the mathematical model of the process from the control point of view, thus to model the heat transfer during the nitriding, to develop the treated part's temperature and the pressure's dynamic equations. The obtained model is used in the followings to design a model-based process controller.

The paper is organized as follows. In Section 2, the DCPN process is described and the heat transfer is modelled. The mathematical model of the thermal process contains temperature dependent parameter, namely the emissivity of the steel, in this chapter a new emissivity estimation method is developed and validated. In Section 3, the dynamic model of the process is developed and the adaptive model-predictive controller is designed, the simulation results are presented. Section 4 contains the conclusions. Section 5 contains the modelling example for the laboratory plasma nitriding system.

2. HEAT TRANSPORT MODELLING

The plasma nitriding takes place in a vacuum chamber, a possible setup is presented in Fig. 1. This chamber has a linear gas flow, the gas mixture enters in the chamber at the top while the vacuum pump is on the bottom. The wall of the chamber is the anode and the treated part is the cathode in the case of DCPN. The wall of the chamber is cooled with water, and there is a Langmuir probe feedthrough for plasma diagnostic purposes.

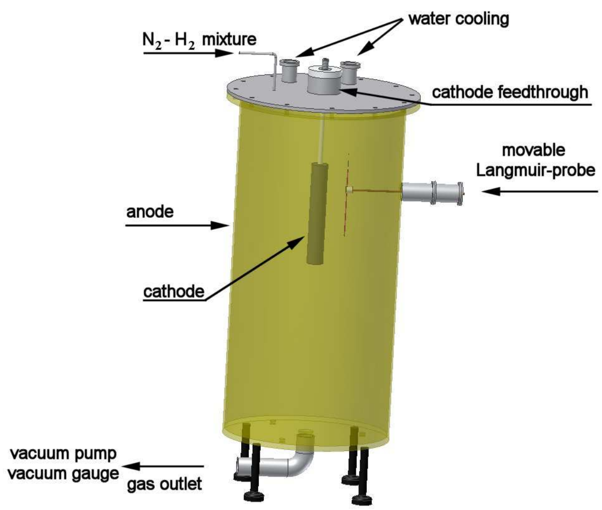

Fig. 1. Linear, non-isotherm plasma reactor used for direct current plasma nitriding.

The schematic principle of the system is presented in Fig. 2.

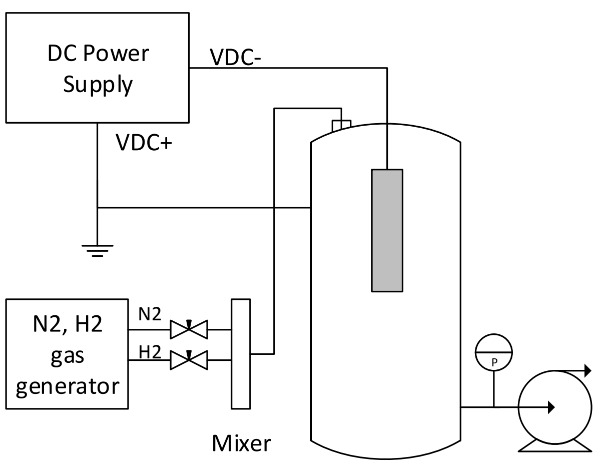

Fig. 2. The plasma nitriding system consisting of the plasma reactor, the DC power supply, the gas supply and the vacuum pump.

The plasma reactor is supplied with a high voltage, controlled DC power supply and a N_2-H_2 gas generator. The N_2 and H_2 gas flow is controlled by the generator, the necessary gas mixture is obtained using a mixer. The working pressure in the chamber is given by the inlet gas flow and the pumping speed of the vacuum pump.

In the presented setup the cathode is the treated part, thus the heating of the part to the required temperature (usually 810K-873K) and the glow discharge is controlled by the DC power supply. The heat transfer from the part has three mechanisms. The continuous gas flow through the reactor transfers a certain amount of heat from the part to air through the vacuum pump. The second heat transfer mechanism is the heat conduction in radial direction from the part to the cooled chamber wall. The third and most important heat transfer is through radiation. In the followings the mathematical model of the heat transfer is developed.

2.1 The heat transport by the gas flow

To determine the heat power transported by the gas, it is necessary to know the absolute gas amount. The gas amount can be calculated using the ideal gas low (1), written to the inlet gas flow or to the outlet gas flow. In this case the outlet gas flow is used, due to the fact that the outlet gas pressure is measured.

$$pV = \nu RT \quad \Rightarrow \quad \nu = \frac{pV}{RT} \qquad (1)$$

In (1) p is the pressure of the outlet gas (Pa), V is volume of the gas (m^3), ν is the amount of gas (kmol), R is the ideal gas constant (8310 J/kmolK), T is the temperature of the outlet gas (K). Taking the time derivative of (1)

$$\frac{d\nu}{dt} = \frac{p}{RT}\frac{dV}{dt} \qquad (2)$$

the mass flow of the gas is obtained (kmol/s). The heat power transported by the gas flow is given by (3),

$$P = \frac{d\nu}{dt} C_p \Delta T \qquad (3)$$

where P is the power (W), Cp is the heat capacity of the gas (for diatomic gas is $7R/2$) and ΔT is the temperature rise of the gas. Equation (3) will be used in the power equilibrium equation, in the dynamical model of the system.

2.2 The heat transport by conduction

The thermal conductivity of a gas depends on the nature of the gas and the temperature. The conductivity of a gas mixture is not exactly the weighted average of the component's conductivity, however in the following model it is considered as the average due to the lack of this data, (Hermann, 1986). The typical thermal conductivity of the N_2, H_2 and the calculated mixture's conductivity for different temperatures are presented in Table 1. The heat flow in the cylindrical chamber in radial direction is given by the Fourier first law,

$$P = -\lambda 2\pi rh \frac{dT}{dr} \qquad (4)$$

where, λ is the averaged thermal conductivity, r is the distance measured in radial direction from the centre of the chamber, h is the high of the cathode, dT/dr is the radial temperature gradient.

Table 1. Thermal conductivity values λ(W/mK)

Temperature (K)	H_2	N_2	$25\%N_2+75\%H_2$
273	0.1593	0.0243	0.1256
373	0.1999	0.0305	0.1576
473	0.2352	0.0362	0.1854
573	0.2666	0.0410	0.2102
673	0.2951	0.0455	0.2306
773	0.3214	0.0497	0.2534
873	0.3458	0.0535	0.2727

From (4), separating the variables,

$$dT = -\frac{P}{\lambda \cdot 2\pi \cdot h}\frac{dr}{r} \tag{5}$$

and defining the limits of the integration as: at the cathode R_1 –> T_1, at the anode R_2 –> T_2 and in general r –> T, from (5) results:

$$\int_{T_1}^{T} dT = -\frac{P}{\lambda 2\pi h}\int_{R_1}^{r}\frac{dr}{r} \quad \Rightarrow \quad T - T_1 = -\frac{P}{\lambda 2\pi h}\ln\frac{r}{R_1} \tag{6}$$

From (6), the conducted heat power results:

$$P = \frac{\lambda 2\pi h}{\ln\frac{R_2}{R_1}}\left(T_1 - T_2\right) \tag{7}$$

Equation (7) will be used in the power equilibrium equation, in the dynamical model of the system.

From (7) and the definitions used in (5), it is possible to determine the temperature distribution in radial direction. From (7), the temperature at distance r from the centre is:

$$T = T_1 - \frac{P}{\lambda 2\pi h}\ln\frac{r}{R_1} \quad where \quad r \in \left[R_1, R_2\right]. \tag{8}$$

The average temperature in radial direction according to the definition is:

$$\langle T\rangle = \frac{1}{R_2 - R_1}\int_{R_1}^{R_2} T(r)dr \tag{9}$$

2.3 The heat transport by radiation

The heat transfer by radiation is quantitatively the most important power loss in the system. The radiated power is described by:

$$P = \sigma S\left(e_1 T_1^4 - e_2 T_2^4\right), \tag{10}$$

where e_1 is the emissivity of the part and e_2 is the emissivity of the chamber's wall, S is the surface of the cathode (the part) and σ is the Stefan-Boltzmann constant. The emissivity of the part is temperature dependent variable, to be able to develop an accurate model, it is necessary to obtain the equation of temperature dependence of the emissivity.

2.4 Estimation of the emissivity versus temperature

There are two methods described in the literature to determine the emissivity of steel at high temperatures, (Paloposki, 2005). The first method, called SP method is expensive and can be performed in laboratory environment, while the second method called VTT is simple but it needs an oven to heat up the part and temperature recorder to determine the emissivity. In the followings we propose an exact method to estimate the emissivity of steel using the plasma nitriding equipment (Fig.2), without any external measurement device.

The emissivity estimation has the following principle. Using the Plasma nitriding equipment, the investigated part is heated up to 830K, using the nitriding conditions. When the temperature equilibrium is obtained, the gas feeding is closed then the electrical supply is also interrupted. All residual gases are evacuated, thus a deep vacuum is obtained. In this condition the cooling speed of the part (cathode) is almost equal to the radiated energy (around 98%), there is a small amount of heat transfer by conduction through the cathode holder and the chamber wall's radiation can be considered also (all together are less than 2%). Recording the cooling curve, the emissivity of the part can be estimated. In the first estimation, let's consider only the radiation, thus the energy balance for the part having the mass of m (kg) is:

$$mc\frac{dT}{dt} = e_1\sigma ST^4, \tag{11}$$

thus the emissivity is:

$$e_1 = \frac{mc\frac{dT}{dt}}{\sigma ST^4}. \tag{12}$$

In the second approach, the heat conduction of the cathode holder (rode with radius R_r, length l) and the chamber's wall radiation is also considered. The heat loss by conduction is given by the Fourier first law (λ_R is the heat conduction of the road), thus:

$$Q_2 = \frac{\lambda_r \pi R_r^2}{l}\left(T_1 - T_2\right), \tag{13}$$

while the radiation of the chamber wall can be expressed as:

$$Qw = e_2\sigma ST_2^4. \tag{14}$$

From (11),(13),(14) results the total energy balance:

$$e_1\sigma ST_1^4 = mc\frac{dT}{dt} + e_2\sigma ST_2^4 - \lambda_r \pi R_r^2\left(T_1 - T_2\right), \tag{15}$$

the emissivity of the treated part for a given temperature results:

$$e_1 = [mc\frac{dT}{dt} + e_2\sigma ST_2^4 - \lambda_r \pi R_r^2\left(T_1 - T_2\right)]/(\sigma ST_1^4) \tag{16}$$

Using (16) and the method described above, in the followings the emissivity of a C45 carbon steel is determined (for the parameters of the system and the experiment see Section 5). The temperature of the chamber's wall is considered constant (T_2) due to the fact that it is cooled with cooling water. In Fig.3 the recorded cooling curve is presented.

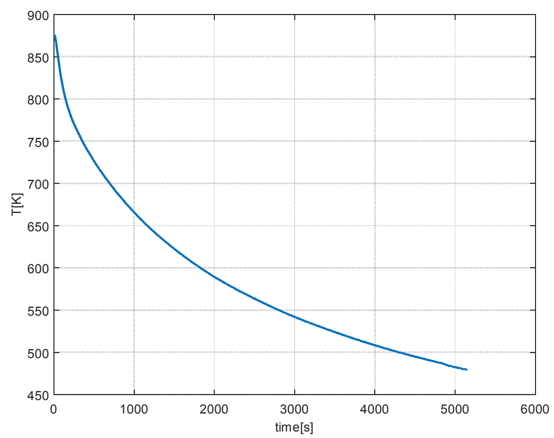

Fig. 3. The cooling curve of the investigated part (from 873K).

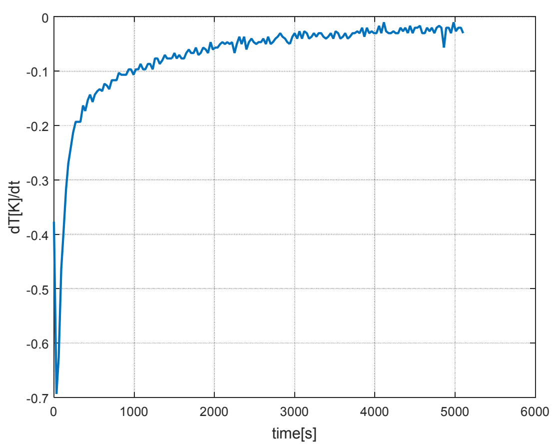

Fig. 4. The derivative of the cooling curve.

Using (16) and the derivative of the cooling curve (Fig.4), the emissivity of the part results as in Fig.5. It is important to notice that the emissivity of the investigated part is highly temperature dependent, the emissivity value is doubled in the 300K-873K temperature range. The obtained function is nonlinear, thus in the mathematical model of the system, the emissivity will be approximated with a third order function:

$$e\_est(T_1) = a_1 T_1^3 + a_2 T_1^2 + a_3 T_1 + a_4 \tag{17}$$

(In eq. (17) $a_1 = 6.09 \cdot 10^{-9}$, $a_2 = -3.43 \cdot 10^{-6}$, $a_3 = 3.67 \cdot 10^{-4}$, $a_4 = 3.55 \cdot 10^{-1}$).

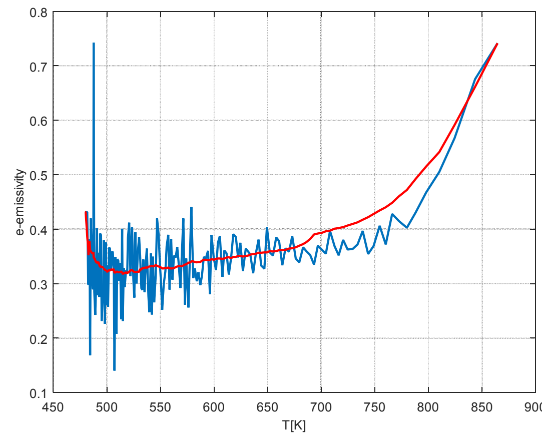

Fig. 5. The estimated emissivity and its filtered values versus the temperature.

3. DYNAMIC MODEL OF THE SYSTEM

From technological and control point of view, there are two process variables that need exact model, the temperature of the treated part end the pressure of the gas mixture in the chamber. In the followings the development of the continuous differential equations describing the temperature and pressure dynamics are presented.

The dynamics of the treated part's temperature results from the heat-power equilibrium equation. The heat quantity necessary to heat up the part with ΔT is:

$$Q = m \cdot c \cdot \Delta T , \tag{18}$$

where m (kg) is the mass off the part and c (J/kgK) is the specific heat. The heating power is given by the derivative of (18), thus:

$$P = \frac{dQ}{dt} = m \cdot c \cdot \frac{dT}{dt} \tag{19}$$

The effective heating power is the difference between the introduced power and the power loss, thus:

$$\frac{dT}{dt} = \frac{1}{m \cdot c} \cdot \left[P_{in} - P_g - P_c - P_e \right] \tag{20}$$

where:

- $P_{in} = U \cdot I$ the introduced electrical power
- $P_g = \frac{d\nu}{dt} C_p \left(\langle T \rangle - T_2 \right)$ the heat-power transported by the gas flow (3)
- $P_c = \frac{\lambda 2 \pi h}{\ln \frac{R_2}{R_1}} \left(T_1 - T_2 \right)$ the heat transported by conduction (7)
- $P_e = \sigma S \left(e_1 T_1^4 - e_2 T_e^4 \right)$ the radiated heat power (10)

Substituting in (20) the expression of each heat-power component, the differential equation of the heating is obtained:

$$\frac{dT_1}{dt} = \frac{1}{m \cdot c} \cdot \left[\begin{array}{l} U \cdot I - \frac{d\nu}{dt} C_p \left(\langle T \rangle - T_2 \right) - \frac{\lambda 2\pi h}{\ln \frac{R_2}{R_1}} \left(T_1 - T_2 \right) - \\ - \sigma S \left(e_1 T_1^{\,4} - e_2 T_2^{\,4} \right) \end{array} \right] \tag{21}$$

The second control variable is the pressure of the gas mixture in the chamber. The parameters that influence the pressure in the reactor are presented in Fig.6. The inlet gas flow (Q_v) is considered after the gas mixer (see Fig.2), while the outlet gas flow is determined by the pumping speed of the vacuum pump (S_p).

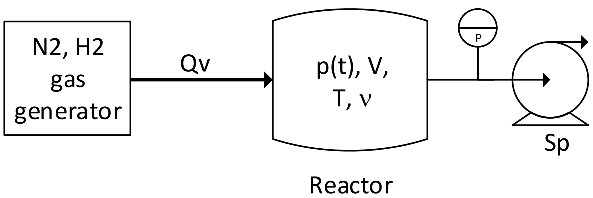

Fig. 6. Gas-feeding of the reactor, the inlet gas flow, the parameters that influence the pressure in the chamber and the pumping speed of the vacuum pump.

The ideal gas law for the reactor, according to (1) is:

$$pV = \nu RT \tag{22}$$

There are two variables in (22), the pressure of the gas mixture (p) and the gas amount (ν), thus the time derivative of (22) become:

$$\frac{dp}{dt} = \frac{d\nu}{dt} \frac{RT}{V} \tag{23}$$

There are two reasons for the $d\nu$ change in the gas amount, first the $d\nu_1$ gas amount change due to the inlet gas flow (Q_v), while the $d\nu_2$ gas amount change due to the pumping (S_p). Considering (23) for the inlet gas flow:

$$p_1 Q_v = \frac{d\nu_1}{dt} RT \tag{24}$$

and for the outlet gas flow:

$$pS_p = \frac{d\nu_2}{dt} RT \tag{25}$$

The pressure of the inlet gas (p_1) is considered as normal pressure and the temperature of the inlet gas (T) is considered the same as the gas temperature in the reactor due to the constant cooling of the reactor.

From (24), (25) and (23) results the differential equation of the pressure dynamics in the reactor:

$$\frac{dp}{dt} = (p_1 Q_v - pS_p) \frac{1}{V} \tag{26}$$

Equation (21) and (26) describe the dynamics of the system. From control point of view, it is better to consider as input variable the applied voltage, thus the modelling of the current is also necessary. According to (Kaptzov, 1956), the current in a DC plasma discharge can be expressed from:

$$U = U_n + \frac{k}{p} \cdot (I - I_n)^{1/2} \tag{27}$$

Where U is the applied DC voltage, U_n is the minimum voltage level which assure the complete cover with discharge of the cathode, I is the current corresponding to U, I_n the current corresponding to U_n, p is the pressure in the reactor and k is an empirical, temperature dependent parameter. From (27) and considering k temperature dependent, the DC current results as:

$$I = \left(\frac{(U - U_n) \cdot \frac{p}{T}}{k'} \right)^2 . \tag{28}$$

The validation of the model for the experimental setup is presented in Section 5.

4. CONTROLLER DESIGN

The industrial DCPN equipments are equiped with PID controllers for the temperature control. A well tuned controller can assure satisfactory control performance for a given temperature setpoint and a given load parameter. In the hardening workshops, the duty of the reactor is varying depending on the requested amount of hardening, thus the m – mass is vary, the emissivity of the part is also vary depending on the composition of the steel, the total surface S of the hardened part is changing as well. As a consequence, it is hard to design a controller with fixed parameters that can meet the desired control performance. Analyzing the model of the system, equation (21) is nonlinear and parameter varying due to the thermal radiation and the above presented varyations in the process, the second component of the model (26) is linear. In the following an adaptive model based predictive controller design is presented in order to overcome the nonlinearity and parameter variation problems.

Model predictive control has become a reliable solution to control problems where the model of the system is known, there are constraints on the model variables and an optimal solution is required. In case of nonlinear model or/and model with parameter uncertainties there are two typical ways to obtain online linear models, to use successive linearization or to implement an online linear model estimator. For details on adaptive MPC and nonlinear MPC, see (Tanaskovics et al., 2013), (Nisha et al., 2015), (Bavili et al., 2015), (Mathworks, 2015).

For the DCPN process, the control variables are the temperature of the treated part and the pressure of the gas mixture, the inputs are the applied DC voltage and the gas flow. Thus the linear, but parameter varying system's state-space model can be considered as a MISO (Multi-Input Single Output) discrete model, according to (29). The output is considered the temperature, while the pressure is considered as a disturbance variable due to the fact, that the process works at constant pressure given by the gas generator and vacuum pump (there is no control possibility in the experimental setup, only manual adjustments are possible).

$$\begin{cases} \begin{pmatrix} T(t+1) \\ p(t+1) \end{pmatrix} = A(t) \cdot \begin{pmatrix} T(t) \\ p(t) \end{pmatrix} + B(t) \cdot \begin{pmatrix} U(t) \\ q(t) \end{pmatrix} \\ y(t) = C \cdot \begin{pmatrix} T(t) \\ p(t) \end{pmatrix} \end{cases} \tag{29}$$

The actual system matrix (*A(t)*) and input matrix (*B(t)*) are estimated using Kalman filter, first an ARX regression model (30) is estimated followed by an ARX-SS model transformation.

$$y(t) + A_1 \cdot y(t-1) + A_2 \cdot y(t-2) + \ldots + A_{na} \cdot y(t-na) = B_0 \cdot u(t) + B_1 \cdot u(t-1) + \ldots + B_{nb} \cdot u(t-nb) + e(t) \tag{30}$$

where *y(t)* is the output, *u(t)* is the input and *e(t)* is a white noise.

The adaptive MPC solves to optimal control problem in a receding horizon manner, using the actual estimated model for the prediction of the future states. The principle of the adaptive MPC of the DCPN process is presented in Fig.7.

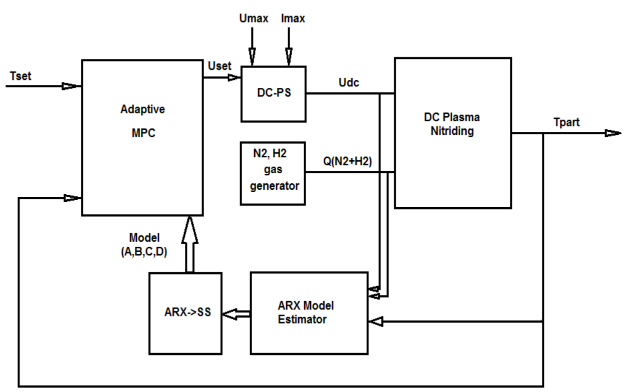

Fig.7. Block-diagram of the proposed adaptive MPC.

The design parameters of the MPC are:

– N_u=2, the control horizon
– N_y=10, the prediction horizon
– Quadratic cost function with waighing *R*=0.1*I and *Q*=I (I-identity matrix).
– Constraints U_{max}=1000V, U_{min}=150V

The parameters of the system for the simulations are:

– *m*=2.94kg
– *Qin* =2*10^{-5} l/min.
– T_2=300K.

The simulation results of the adaptive MPC are compared with a well tuned PID with anty-windup, the simulation results are presented in the following figures.

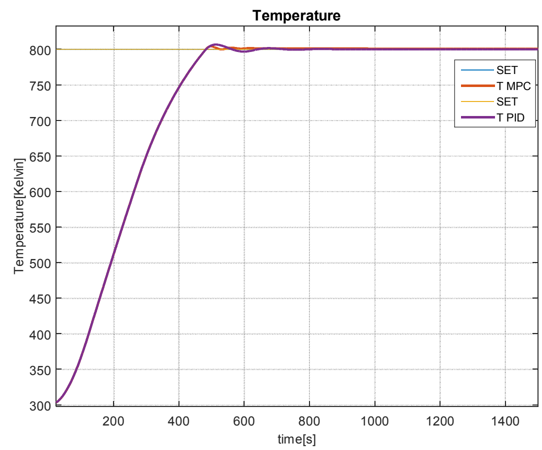

Fig.8. Temperature control in case of step change in the setvalue (800K). The adaptive MPC has a shorter settling time and lower overshot, but both controllers perform well.

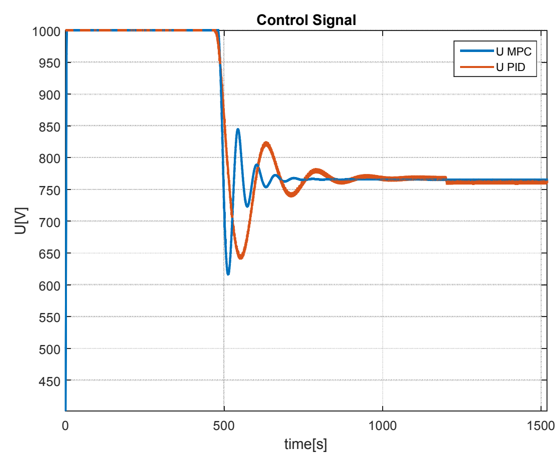

Fig.9. Control signal (input voltage) in case of step change in the setvalue.

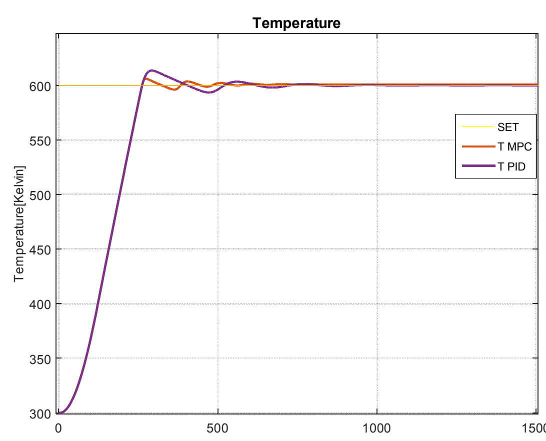

Fig.10. Temperature control in case of step change in the setvalue (600K). In this example the benefit of the adaptive MPC is evident.

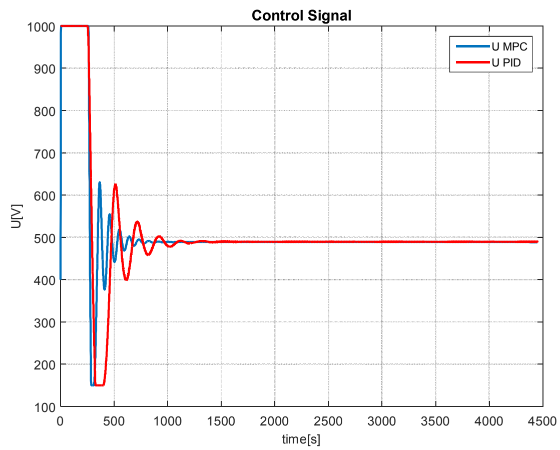

Fig.11. Control signals in case of step change in the setvalue (600K).

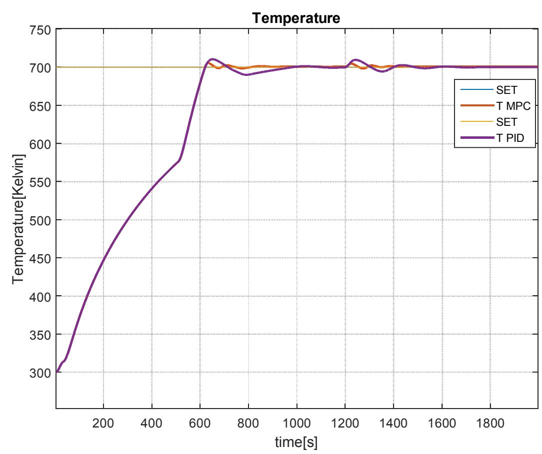

Fig.12. Temperature control in case of 700K setvalue and gas-flow perturbation.

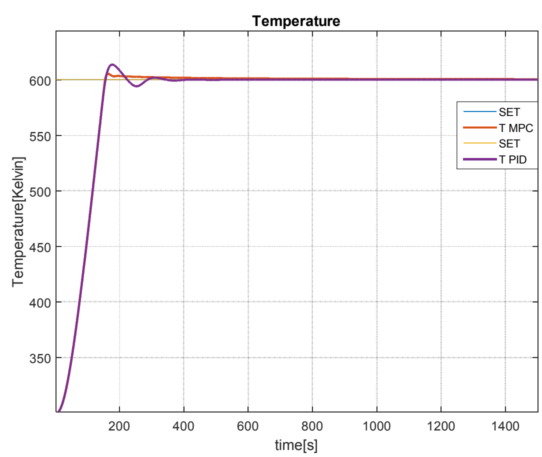

Fig.13. Temperature control in case of change in the mass of the treated part, the total mass has been reduced from m=2.94 kg to m=0.94kg. The adaptive MPC is "immune" to the parameter change, while the PID have a higher overshot.

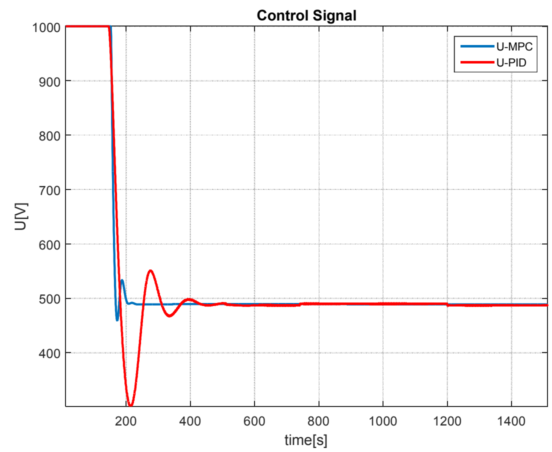

Fig.14. Control signal in case of load change.

In Fig.12 at 500s, the inlet gas flow has doubled to $Qin=2*10^{-5}$ l/min, at 800s the flow became $Qin=10^{-5}$ l/min and at 1200s $Qin=2*10^{-5}$ l/min. The adaptive MPC has a better performance in perturbance rejection.

The simulation results show a clear benefit of the adaptive MPC compared to the PID controller, however it is difficult to implement due to the optimization and estimation algorithms.

5. EXPERIMENTAL SETUP

In this section the experimental setup is presented, the parameters of the system and the model validation are described.

Fig. 15. The experimental setup consisting of the plasma reactor, the DC power supply, the gas generator, vacuum pump and a PC for process control.

The parameters of the system:

- Reactor:
  - Ø=247mm inner diameter (R_2=0.247/2)
  - l=1000mm, made from aluminum, with double wall (for cooling)

- cathode rode made of a $\O$=12mm steel, isolated ($Rr=6\cdot10^{-3}$ m)
- volume V=50 liter.
- The temperature of the wall T_2=300K.
- Emissivity of the wall e_2=0.3

– Vacuum pump with pumping capacity $S_p = 4{,}17\cdot10^{-3}$ m^3/s

– Inlet gas flow and composition Qv=150 mL/mn N_2+450 mL/mn H_2, the steady gas pressure in the chamber is p=250 Pa.

– Test part:
- m=2.94 kg.
- h=0.204m
- R_1=0.0485/2 m
- S=0.03721 m^2

– DC Power supply:
- Rated power 2.2 kW
- U_{max}=1200V
- I_{max}=2000mA
- Digital control, arc management

– Constants used in the equations:
- R=8310 J/kmolK
- $\sigma=5.67\cdot10^{-8}$ W/(m^{2}K^4)
- c_{Fe} = 460 J/(kgK)
- λ_R = 16 W/(mK) – for the rod
- λ= 0.2 W/(mK) – for the gas mixture
- C_p=7R/2

For the validation of the mathematical model, the step response of the experimental setup and the simulation was examined. The registered temperature, voltage and current curves were compared. In the first step, the working pressure of the reactor was set to 250Pa and the power supply was started in arc management mode, to clean the workpiece. This behavior can be observed in the first 700s. In the recorded voltage curve several start/stop (arc discharge) can be observed. Thus the effective heating of the part take place from 700s, thus the simulation was made in the same manner. The applied voltage was 600V.

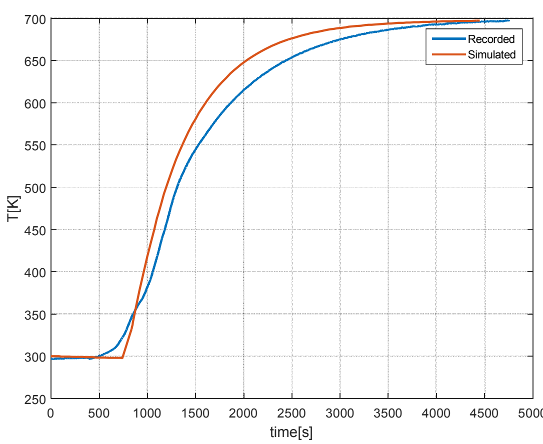

Fig. 16. The evolution of the temperature in case of a 600V step input. The upper (red) curve is the simulated, the blue one is the recorded temperature.

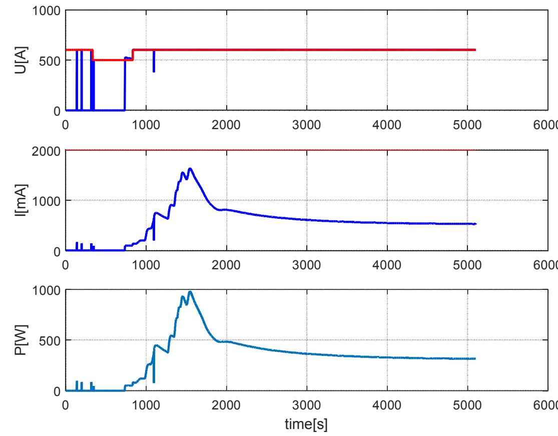

Fig. 17. The recorded voltage, current and power values.

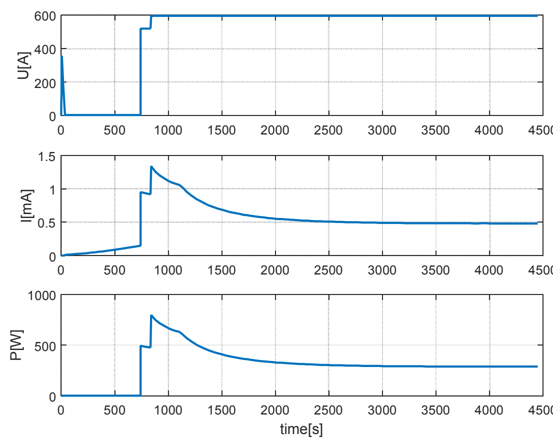

Fig. 18. The simulated voltage, current and power values.

The heat-power values for a certain cathode temperature and a constant cooling of the reactor has been determined and the effect of the different heat conduction mechanism was examined. The cathode temperature was considered T_1=873K and the wall of the reactor T_2=300K.

According to (3) the transported heat-power depends on the pressure, in this case p=245Pa, the temperature of the outlet gas, T=300K and the mass flow rate (2):

$$\frac{d\nu}{dt} = \frac{245}{8310\cdot300}\cdot 4.17\cdot10^{-3} = 4.09\cdot10^{-7}\,\text{kmol/s} \qquad (31)$$

Thus the calculated heat loss, for a ΔT=210K temperature rise of the gas around the cathode become:

$$P_g = \frac{d\nu}{dt}C_p\Delta T = 4.09\cdot10^{-7}\,\frac{7}{2}\cdot8310\cdot210 = 2.495\,W \qquad (32)$$

The second component of the heat loss is the conducted heat, according to (7):

$$P_c = \frac{\lambda 2\pi h}{\ln\frac{R_2}{R_1}}(T_1 - T_2) = \frac{0{,}2\cdot6{,}28\cdot0{,}22}{\ln\frac{247}{48{,}5}}(873-300) = 97\,W \qquad (33)$$

The most significant heat loss is due to the radiation (10):

$$P_e = \sigma S\left(e_1 T_1^4 - e_2 T_2^4\right) =$$
$$= 5{,}67 \cdot 10^{-8} \cdot 0{,}03721 \cdot \left(0{,}71 \cdot 873^4 - 0{,}35 \cdot 300^4\right) = 855\,W \qquad (34)$$

In conclusion, according to (32), (33), (34) the radiated heat loss is around 80-90% of the total loss, the conduction has a 10-15% from the total loss, while the heat transported by the gas-flow is less than 1%.

6. CONCLUSIONS

The paper is dedicated to modelling and control of the direct current plasma nitriding process. The developed model can be used for simulation and controller design, the developed model can be adapted to any configuration of reactor and gas feeding. The model based control of the process is dificult due to the nonlinearities and parameter variation, thus an adaptive model based controller is proposed, where the model of the system is estimated. The obtained controller's performance has been compared to a well known PID controller, for different parameter and setvalue configurations.

REFERENCES

Bavili, R.E. and Khosrowjerdi, M.J. (2015) Active Fault Tolerant Controller Design using Model Predictive Control, *Journal Of Control Engineering And Applied Informatics*, Vol. 17, No.3, pp.68-76

Cavaliere, P.,Zavarise G. and Perillo M.(2009) Modeling of the carburizing and nitriding processes, *Computational Materials Science* 46 (2009), pp. 26–35

Filetin T., Žmak I., Lisjak D., Novak D. and Landek D. (2005) The application of artificial intelligence methods in heat treatment. *1st international conference on heat treatment and surface engineering of tools and dies IFHTSE*. Pula, Croatia, p. 469-476.

Guiberteau, E., Bonhomme, G., Hugon, R. and Henrion. G. (1997) Modelling the pulsed glow discharge of a nitriding reactor, *Surface and Coatings Technology* 97 (1997) pp.552–556

Hermann, E. Physikalisches Taschenbuch, *Friedr. Vieweg & Sohn: Braunschweig*, 1986

Kaptzov, N.A. (1956) Electronica. Ed.Tehn. Bucuresti, P.293

Kenez, L., Kutasi, N. Filep, E., Jakab, L.F. and Szocs, I.A.(2013) HeatTreatment of 16MnCr steel in a linear non-isoterm plasma reactor, *Acta Universitatis Sapientiae, Electrical and Mechanical Engineering*, 5, pp. 61-72.

Mittemeijer, EJ. (2013) Fundamentals of Nitriding and Nitrocarburizing. Steel *Heat Treating Fundamentals and Processes, ASM Handbook*, 2013; 4(A):619-646.

Mathworks (2015) Adaptive MPC - http://www.mathworks.com/help/mpc/ug/adaptive-mpc.html#

Nisha, M.G. and Pillai, G.(2015) Nonlinear model predictive control of MIMO system with Least squares support vector machines and Particle swarm optimization, *Journal Of Control Engineering And Applied Informatics*, Vol. 17, No.4, pp.14-22

Oltean, S.E. and Dulau, M. (2014) Design and Simulation of Fuzzy Logic Based Temperature Control for a Plasma Nitriding Process, *8th International Conference Interdisciplinarity in Engineering, INTER-ENG 2014*, 9-10 October 2014, Tirgu Mures, Romania, Procedia Technology Volume 19, 2015, Pages 569–575

Paloposki, T. and Liedquist, L. (2005) Steel emissivity at high temperatures, VTT Tiedotteita – research note 2299 (http://www.vtt.fi/inf/pdf/tiedotteet/2005/T2299.pdf)

Ratajski, J. and Suszko, T. (2008) Modelling of the nitriding process, *Journal of materials processing technology* 195 22(2008) pp. 212–217

Ratajski, J., Olik, R., Suszko,T.,Dobrodziej, J., Michalski, J. and Gilewicz A. (2009) Precise formation the phase composition and the thickness of nitrided layers *Journal of Achievements in Materials and Manufacturing Engineering*, 37 (2), pp. 675–689

Rembges, W. and Oppel, W. (1993) Process control of plasma nitriding and plasma nitrocarburizing in industry, *Surface And Coating Technologies*, Vol 59. Issues 1-3.

Satyapal, M., Khanna, A.S., Alphonsa, J. (2013) Effect of Temperature on the Plasma Nitriding of Duplex Stainless Steels, *International Journal of Engineering and Innovative Technology (IJEIT)*, 2 (11) , pp. 217.

Tanaskovic, M., Fagiano, L., Smith, R. and Morari, M. Adaptive receding horizon control for constrained MIMO systems. *Automatica*, 2013.